25th ABCM International Congress of Mechanical Engineering
October 20-25, 2019, Uberlândia, MG, Brazil

COB-2019-1235 HEAT TRANSFER IN LARGE RUBBER ELEMENTS THROUGH OF MODELING BY FINITE DIFFERENCE METHOD

Lucas Palmeira Peixoto
Ane Lis Marocki
Celso Vieira Junior
Viviana Cocco Mariani
Department of Mechanical Engineering (PPGEM), Pontifical Catholic University of Parana (PUCPR)
Rua Imaculada Conceição, 1155, Curitiba, PR, Brazil

e-mails: lucaspalmeirapeixoto@gmail.com, ane.marocki@gmail.com, c.vieira_10@hotmail.com, viviana.mariani@pucpr.br

Abstract. *Rubber is a typical viscoelastic polymer and has a low thermal conductivity. The main consequence is heat generation and leads to a temperature rise called heat build-up of the rubber material* when subjected to cyclic deformation. *Numerical modelling to predict the physical processes of heat transfer, typically complicated, in the curing of rubber using the finite difference method are presented in this study. The transport phenomena during curing of rubber was modeled using basic equations without considering the values and variation in the shrinkage stress and strain. One code developed with the Python open source language and its mathematical libraries, was proposed in this study and applied to solve this problem. The numerical results agreed with simulations presented previously in literature. The deviation obtained for temperature values is around 1% in the heating and cooling phases when comparing with results of the literature. Future work should include shrinkage model and solve the more complicated equations about heat and mass transfer considering the water concentration variation to improve the formulated model. The inclusion of the vapor phase in the drying air would also help improve the physical model.*

Keywords: *Finite difference method, Cure process, Rubber, Heat transfer.*

1. INTRODUCTION

Heat transfer is a widely used tool for solving engineering problems as well as for the development and evaluation of the performance of various materials, among them rubber (White, 2005). This material is famous in the industry due to its high deformation capacity and durability. It has application in several sectors such as medical; aerospace; civil construction; military and others. An important process in the manufacture of rubber elements is the curing step, in the study of Abhilash *et al.*, (2010) shows that rubber subjected to a non-uniform thermal history showed a non-uniform curing process, which made it is mechanical properties non-uniform, therefore a non-homogeneous material. It is essential to obtain the optimum curing temperature due to it is influence on the final physical properties of the material. When it comes to small parts obtaining the temperature is easy to perform. However, some rubber applications require large parts, but the determination of the curing temperature in larger elements represents a great challenge for industry due to the existence of temperature gradients during much of the curing process, thus it is very important to apply a method for determining the temperature at various points of large rubber elements.

As mentioned previously, the determination of the optimum curing time is essential for the controlling of the resulting mechanical properties in the production of thick rubber particles. However, its experimental determination is an expensive and time-consuming process, as a result numerical solution are commonly employed in industry according to Erfanian *et al*. (2016). A breve review of the literature on the rubber curing process as well as some mathematical models and simulations applicable to this process are present, for example, in the study of Ghoreishy *et al*. (2016). Therefore, among the main methods used to carry out this type of simulation, it is worth mentioning in Limrungruengrat *et al*. (2018) using the software RACE-CURE and the commercial ABAQUS to simulate the vulcanization process in a large rubber part. In Rafei *et al.,* (2009)'s work is purposed simultaneously solve the heat conduction equation and the rubber cure kinetics, the general finite element code Abacus was used in conjunction with an internal subroutine (UMATHT). Another way of obtaining the heat transfer process was presented in the study of Yau *et al*. (2012) which used finite difference method (FDM) and later Dolkun (2018) applied the FDM using the Pareto curve to obtain the optimized temperature profiles.

A CFD simulation and experimental investigation of natural rubber sheets drying was performed for a new rubber smoking room design by Dejchanchaiwong *et al*. (2017). CFD simulation was used to solve turbulent 3D flow field along with conjugate heat and mass transfer in rubber sheets. Experimentally, temperature distributions inside the rubber

smoking room and sheet moisture content were measured. The CFD simulation model agreed well with experimental observations. Li *et al*. (2018) introduced effective numerical approach to estimate the transient temperature distribution and rolling resistance of a solid rubber tire. In that work, the strain amplitude was approximated with high accuracy by using the Fourier sine series. The loss modulus was updated as a function of strain amplitude, temperature, frequency and loading cycle. A practical method was proposed to compute the transient temperature distribution and rolling resistance of solid tire by establishing a 2D axisymmetric model. Experimental data verify that the analytical method was a reliable approach. The stable temperature increases with rotating speed and compressive displacement.

Heat build-up of cylindrical rubbers under cyclic loading was experimentally studied and theoretically analyzed based on the heat equation in the work from Luo *et al*. (2018). The effects of loading strain amplitude and frequency on the temperature rise were investigated. The Kraus model and General Maxwell model were employed to establish the relations between loss modulus and strain, frequency of the material, respectively. By considering the effect of rising temperature on loss modulus of rubber material during cyclic deformation, a modified analytical method to predict heat build-up for rubber compounds was proposed. Numerical modelling to predict and experiments to verify the shrinkage behavior of natural rubber sheets under convective drying using the finite element method were presented by Ajani *et al.* (2019). The conjugate approach applied using the virtual work principle on the sheet based on the operating parameter was considered. Shrinkages of about 9.1% were predicted and observed. This shows that the transport phenomena during rubber sheet drying causes shrinkage and cannot be overlooked. The experimental results agreed with simulation.

2. MATHEMATICAL MODELING

2.1 Computational Domain

For computational simulations, the first step is to analyze the computational domain, as it deals with the dimensions and characteristics of the rubber particle and the metal mold particle. We studied two cases, first and fourth cases of the base article, changing the properties of rubber, and we used five different metal molds for each case: (a) steel alloy; (b) bronze; (c) carbon steel; (d) aluminum 2024 – T6; (e) other steel alloy. The physical characteristics of the two types of rubber used and the five metal types used in the computational simulations are shows in Table 1. In the first case studied, Case 1, we have a rubber of 1.68 m of length and 1.18 m of height, surrounded by a metal mold of 2 m od length and a height of 1.5 m. In the second case studied, Case 2, we have a square rubber with 0.1 m sides, while the length and the height of mold is 0.2 m. Figure 1a shows Case 1 explaining the dimensions of the mold/rubber system. Already Figure 1b does the same thing with Case 2

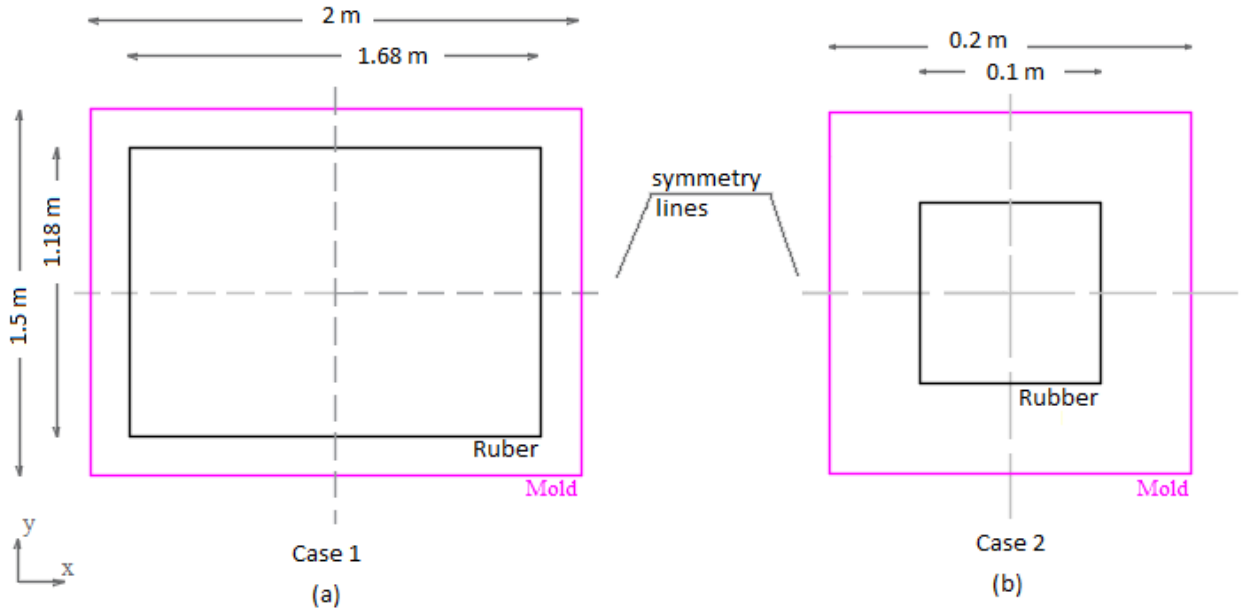

Figure 1 – (a) Case 1 and (b) Case 2.

Table 1 – The physical characteristics of the materials used.

	Rubber - Case 1	Rubber Case 2	Metal - a	Metal - b	Metal - c	Metal - d	Metal - e
Thermal conductivity (W/K.m)	0.24	0.6	60	52	60.5	177	70
Density (kg/m³)	1000	1000	7000	8800	7854	2770	7800
Specific heat (J/kg K)	1600	1600	85	420	434	875	140

2.2 Simplifying Hypothesis

The rubber with the metal mold has a rectangular shape, so we can simplify in order to apply symmetry. Symmetry consists of a relation of parity in respect to the height, width and length of the parts that make up a whole. When heating the mold/rubber assembly, it is possible to apply two symmetries both on the horizontal axis and on the vertical axis. In cooling, was used only the vertical symmetry. Was not used horizontal symmetry in the cooling process because of contour conditions, addressed in section 2.4. Other measures, taken to simplify the problem were to consider the incompressible fluid (Air), 2D computational domain and constant thermodynamic proprieties of all materials.

2.3 Finite Difference Method

It is not always possible to obtain analytical solutions for heat transfer problems, especially in situations of transient regime and elements of geometry; in these cases, the adoption of numerical methods is necessary.

Problem solving by the finite difference method consists of the discretization of the equations. In situations where the regime is transient, the properties of the material remain constant and there is no internal heat generation, the appropriate form presented in Equation 1 below:

$$\frac{\partial T}{\partial t} = \frac{\partial}{\partial x}\left(\frac{k_a}{\rho_a cp_a}\frac{\partial T}{\partial x}\right) + \frac{\partial}{\partial y}\left(\frac{k_b}{\rho_b cp_b}\frac{\partial T}{\partial y}\right) \tag{1}$$

This kind of problem needs to be discretize in space, as showed by Kiusalaas (2013) from the Taylor series the central second order derivative can be obtained and presented in finite difference form, as showed in Equation 2

$$\left.\frac{\partial T}{\partial x}\right|_i = \frac{T^t_{i+1,j} + T^t_{i-1,j} - 2T^t_{i,j}}{(\Delta x)^2} \tag{2}$$

If we substitute Eq. (2) in Eq. (1), the nature of the solution will be dependent on the specific time instant at which the temperatures are determined. In the explicit form, those temperatures are evaluated at the instant of the previous time step. The resulting Equation 3 is the generalized explicit formulation for the finite difference method, without any boundary condition implemented.

$$\frac{T^{t+1}_{i,j} - T^t_{i,j}}{\Delta t} = \alpha\left[\frac{T^t_{i+1,j} + T^t_{i-1,j} - 2T^t_{i,j}}{(\Delta x)^2} + \frac{T^t_{i,j+1} + T^t_{i,j-1} - 2T^t_{i,j}}{(\Delta y)^2}\right] \tag{3}$$

Explaining the temperature of the node in time (p + 1) and considering Δx = Δy, we obtain Equation 4:

$$T^{t+1}_{i,j} = Fo\left(T^t_{i+1,j} + T^t_{i-1,j} + T^t_{i,j+1} + T^t_{i,j-1}\right) + (1 - 4Fo)T^t_{i,j} \tag{4}$$

In which F_o consists of the Fourier number given by,

$$Fo = \frac{k_a}{\rho_a cp_a}\frac{\Delta t}{(\Delta x)^2} \tag{5}$$

2.4 Boundary Conditions

In the present study some boundary conditions were adopted like shown in Figure 1 in section 2.2 and are described in Table 2. The boundary conditions used are prescribed temperature at the point (i.e., Dirichlet boundary condition) for

example between the press and the mold plus rubber assembly; heat flow by convection and conduction on the face performed by an energy balance (Robin boundary condition); discontinuity of flux applied in the change of materials. The symmetry adopted in the heating was applied in both the vertical and horizontal axes. Whereas in the cooling, only the symmetry of the vertical axis was applied, since natural convection occurs in the upper part of the mold as in the lower part with the withdrawal of the press. In the present study are applied several boundary conditions, peculiar to the stage of the curing of the rubber on its heating and cooling processes.

In the heating process, the upper and lower parts of the mold are at a fixed temperature and the boundary condition of Dirichlet is used, its values are presented in Table 2 for both analyzed cases. At the same process the right and left side of que mold are exposed to ambient air, and a convective boundary condition is created, the values of the convective heat transfer used are displayed at table 2 also, for both cases.

At the cooling process, the upper and lower part of the mold no longer possesses a fixed temperature and are exposed to ambient air, consequently, are both involved in a natural convection process. Taking account, the buoyancy effects associated with natural convection, heat transfer constant will appear, as for the right and left side of the mold remains the same and their values are described at Table 3

During both heating and cooling processes, the interface of both materials will present a discontinuity in the heat flow, provided that the thermodynamic proprieties are different. This causes a boundary condition at each point where this discontinuity exists. The equation used to describe this discontinuity is displayed at Tables 2 and 3.

Table 2 – Boundary conditions for the heating process of case 1 and 2.

Heating Processes	Case 1	Case 2
Prescribed temperature at top and lower side (Dirichlet) (^oC)	200	200
Heat flow discontinuity	$-K_a.\frac{\partial T}{\partial x} = K_b.\frac{\partial T}{\partial x}$	$-K_a.\frac{\partial T}{\partial x} = K_b.\frac{\partial T}{\partial x}$
Convection (Robin); h (W/m^2K)	2.5	4.5

Table 3 - Boundary conditions for the cooling process of case 1 and 2.

Cooling Processes	Case 1	Case 2
Natural convection top side; h (W/m^2K)	7.1	7.1
Natural convection lower side; h (W/m2K)	2.6	2.6
Heat flow discontinuity	$-K_a.\frac{\partial T}{\partial x} = K_b.\frac{\partial T}{\partial x}$	$-K_a.\frac{\partial T}{\partial x} = K_b.\frac{\partial T}{\partial x}$
Convection (Robin); h (W/m^2K)	5.7	4.65

3. NUMERICAL RESULTS

Problem solving consists initially in the construction of the mesh, a discrete representation of the domain [a, b], performed by dividing the area of interest into smaller regions with a central reference point for each micro region. The mesh used for the development of this study in the first case was 0.04 m of horizontal and vertical spacing and step time for heating and cooling was 3.8 s. For the second case, the incremental space was 0.0125 m of horizontal and vertical and step time for heating and cooling was 0.6 s Some mesh refining studies have been performed, but no major changes have been observed. Therefore, the mesh adopted in both cases was the one proposed in the base article written by Yau et. al. (2012).

The results of temperature of the heating and cooling processes respectively off the first case are showed in Tables 3 and 4 and the second case displayed at Tables 5 and 6; they portray the percentage difference of the Python simulation using finite difference methods made by the authors and those presented by Yau *et al.* (2012).

The author used the finite difference method and Matlab programing, to compare results with a commercial software Abacus 6.3. This software did not use the same numerical method of the author (Julia, 2007 and Gregory *et al.*, 1999), instead, using a finite element description of the differential equation. Finite element analysis (FEA) can be used to model

heat transfer and thus it can be used to simulate curing of a large rubber object. It is a computer based simulation software technique. It is important to understand, that the method used by the software, is just another mathematical model, therefore their solutions can be compared.

Analyzing the results, it can be seen little difference between the simulations, with a variation less than 1% of the base article values, concluding that the Python code is with good agreement.

Figures 2 and 3 illustrate the results of the Python simulation used in this study. They demonstrate the heating and cooling processes for the first and fourth case of the base article, showed in Figure 2a and 3a, respectively, displaying a similar trend of the base and simulated case, as Table 3 and 4 show an error of less than 1%. Figures 2b and 2c and Figures 3b and 3c, illustrate the temperature map at the end of heating and cooling process, respectively, both with the same behavior presented previously in Yau *et al*. (2012).

The cases used by the author, employed different meshes and thermodynamic proprieties for the rubber and mold. The aim of this change is to generate a better understanding on how the heat flows at the curing process develops. In order to, correctly understand we must analyze two key components: mesh size and thermodynamic proprieties.

The first case has a constant mesh spacing of 0.04 m, which translates to a larger object than case 2, with only 0.0125 m of spacing. This difference directly affects the heat flow of the overall simulation. If we compare the central temperature at the end of cooling process for both cases. Figure 2c shows that core temperature remains constant in rubber in case 1, because is a large object and more energy would be required to alter the temperature. On the other hand, in the case 2 the rubber is much smaller than rubber in case 1. Figure 3c shows the core temperature in the end of heating process is similar to all temperature within the domain for the case 2.

Along with the mesh size, the thermodynamic proprieties used for the mold and rubber are the main influence during the simulation. To analyze the cases 1 and 2, arrays of different materials were used, their thermodynamic proprieties were specified at Table 1.

Table 4 – Temperature (ºC) in heating process for Case 1: comparison on simulation process.

Region	Python	Matlab	Matlab-Python	FEA	Difference FEA
Bottom	198.998	199.014	8.2×10^{-5}	198.969	1.4×10^{-4}
Top	198.998	199.014	8.2×10^{-5}	198.969	1.4×10^{-4}
Side	167.403	167.803	2.4×10^{-3}	167.595	1.1×10^{-3}
Centre	23.000	23.000	5.6×10^{-8}	23.000	5.6×10^{-8}

Table 5 – Temperature (ºC) in cooling process for Case 1: comparison on simulation process.

Region	Python	Matlab	Difference Matlab	FEA	Difference FEA
Bottom	89.869	89.726	1.6×10^{-3}	89.048	9.1×10^{-3}
Top	65.884	65.564	4.9×10^{-3}	65.437	6.8×10^{-3}
Side	73.224	73.727	6.8×10^{-3}	73.424	2.7×10^{-3}
Centre	23.001	23.003	6.7×10^{-5}	23.001	2.0×10^{-5}

Table 6 – Temperature (ºC) in heating process for Case 2: comparison on simulation process.

Region	Python	Matlab	Difference Matlab	FEA	Difference FEA
Bottom	199.231	199.166	3.3×10^{-4}	199.149	4.1×10^{-4}
Top	199.231	199.166	3.3×10^{-4}	199.149	4.1×10^{-4}
Side	197.035	197.776	3.7×10^{-3}	197.695	3.3×10^{-3}
Centre	141.355	141.331	1.7×10^{-4}	140.580	5.5×10^{-3}

Table 7 – Temperature (ºC) in cooling process for Case 2: comparison on simulation process.

Region	Python	Matlab	Difference Matlab	FEA	Difference FEA
Bottom	158.894	158.230	4.2×10^{-3}	158.162	4.6×10^{-3}
Top	156.675	156.964	1.8×10^{-3}	156.807	8.4×10^{-4}
Side	157.795	157.495	1.9×10^{-3}	157.379	2.6×10^{-3}
Centre	171.203	172.081	5.1×10^{-3}	172.455	7.3×10^{-3}

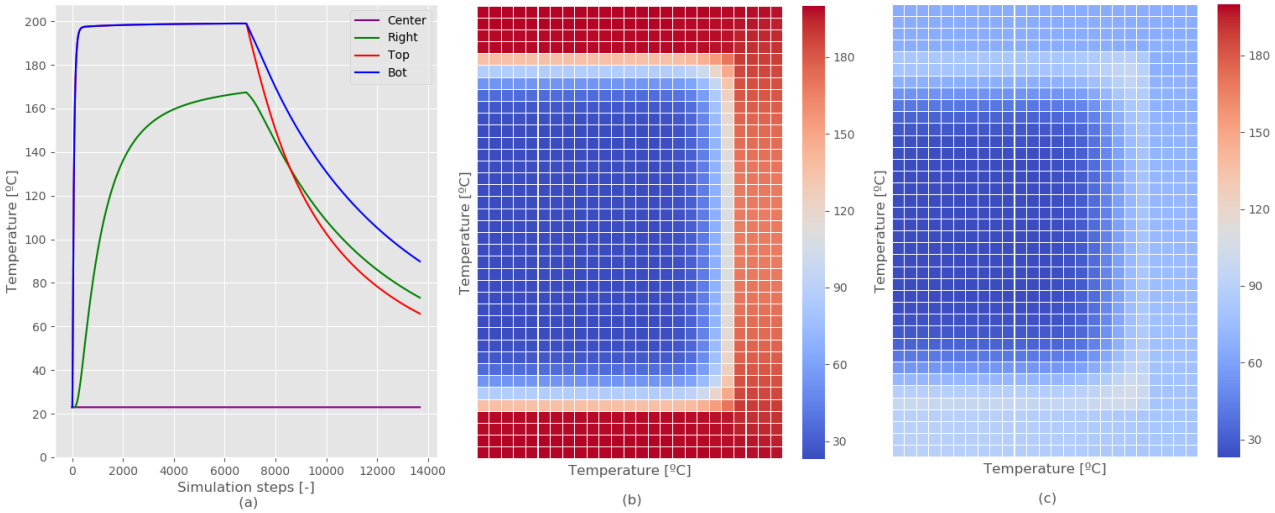

Figure 2 – Case 1 (metal a) - (a) Heating and Cooling process; (b) Temperature map at the end of heating process; (c) Temperature map at the end of cooling process.

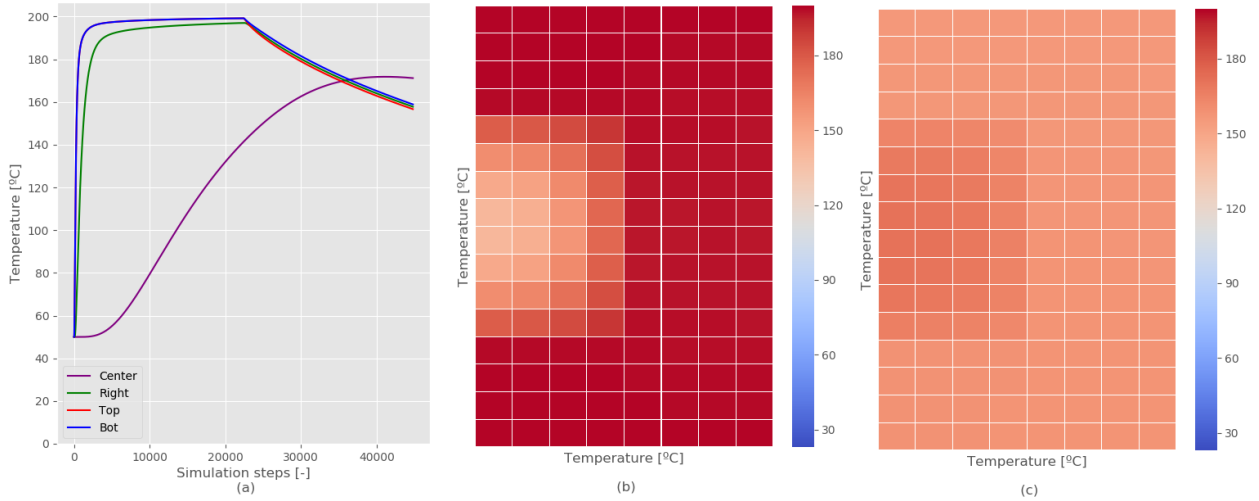

Figure 3 – Case 2 (metal e) - (a) Heating and Cooling process; (b) Temperature map at the end of heating process; (c) Temperature map at the end of cooling process.

After validating the Python code, it was possible to do the simulations changing the metal of the mold. With this, it is possible to observe the good behavior of the Python code with the changes in the physical properties of the metal mold. The good demeanor for the first case of the heating and cooling process, respectively, are show in Table 8 and 9, and for the second case of the heating and cooling process, respectively, was show in Table 10 and 11. In this way, it is possible to simulate any type of material and reduce the need for doing costly laboratorial experiments.

Comparing cases 1 (metal a) and 1 (metal b), is possible to perceive the effect of using a material with different thermodynamic proprieties. Figure 4 shows the case 1 simulation using a bronze alloy as the mold material, that compared with metal a, possesses a higher calorific value and lower thermal conductivity. Figure 4b and 4c display case 1b results of both heating and cooling processes, portraying poor heat flows, as the mold reaches lowers temperatures at the right

side. While maintaining similar temperatures at the top and bottom side. Big changes were fund at the cooling process; case b displayed a higher overall temperature at the end of the process. Extending the same analysis to case 2 (metal a) and 2 (metal b) displayed at Figure 5. Since the mesh is smaller, the maximum temperature is reached and is similar for both cases. As for the cooling phase, the metal b preserves more energy and therefore has a higher temperature of around 20ºC compared with metal a. This form of analyzes can be replicated with all material presented contend in Table 1. This can provide important information when selecting or designing materials. Tabeles 8, 9, 10 and 11 shows the results of cases 1 and 2 with different material.

Table 8 – Comparison of results for Case 1 (heating process).

Region	Metal - a	Metal - b	Metal - c	Metal - d	Metal - e
Bottom	198.998	198.822	198.992	199.661	199.140
Top	198.998	198.822	198.992	199.661	199.140
Side	167.403	128.585	142.865	187.781	170.388
Centre	23.000	23.000	23.000	23.000	23.000

Table 9 - Comparison of results for Case 1 (cooling process).

Region	Metal - a	Metal - b	Metal - c	Metal - d	Metal - e
Bottom	89.869	149.940	147.246	134.197	107.313
Top	65.884	123.881	121.037	114.640	80.922
Side	73.224	117.600	120.749	122.451	89.354
Centre	23.001	23.001	23.001	23.001	23.001

Table 10 - Comparison of results for Case 2 (heating process).

Region	Metal - e	Metal - b	Metal - c	Metal - d	Metal - a
Bottom	199.231	198.800	199.017	199.706	199.107
Top	199.231	198.800	199.017	199.706	199.107
Side	197.035	195.401	196.231	198.836	196.576
Centre	141.355	133.626	136.069	143.490	141.451

Table 11 - Comparison of results for Case 2 (cooling process).

Region	Metal - e	Metal - b	Metal - c	Metal - d	Metal - a
Bottom	158.894	180.529	179.575	174.472	147.314
Top	156.675	177.222	176.674	173.463	144.968
Side	157.795	178.819	178.080	173.960	146.180
Centre	171.203	176.538	177.102	178.151	166.312

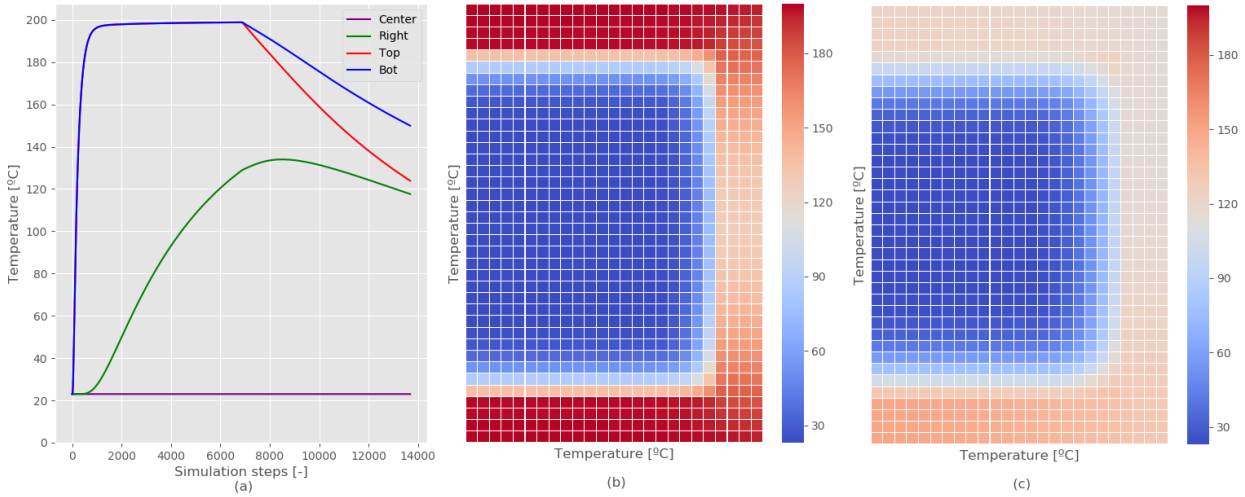

Figure 4 – Case 1 (metal b) - (a) Heating and Cooling process; (b) Temperature map at the end of heating process; (c) Temperature map at the end of cooling process.

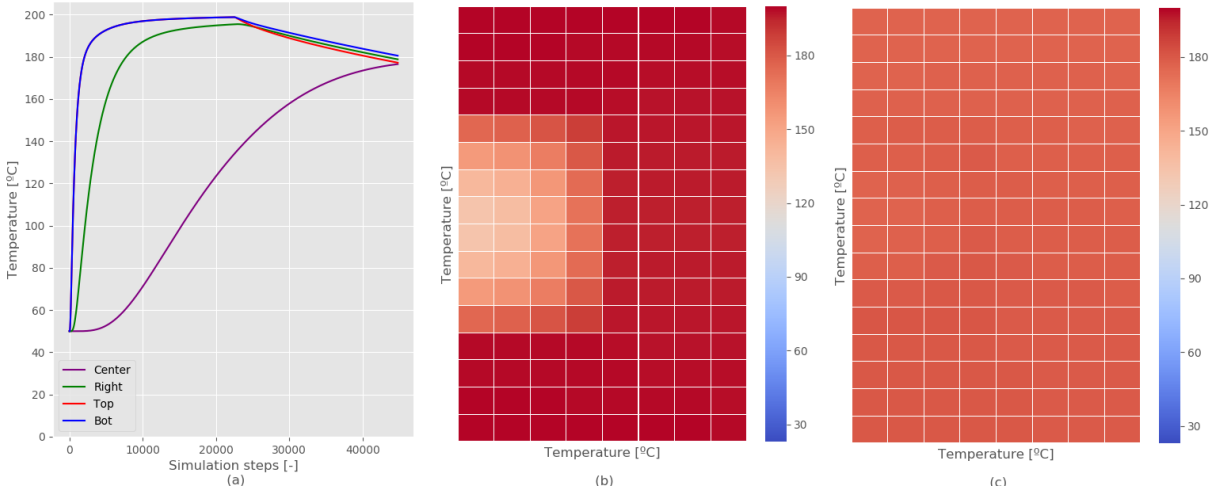

Figure 5 – Case 2 (metal b) - (a) Heating and Cooling process; (b) Temperature map at the end of heating process; (c) Temperature map at the end of cooling process.

4. CONCLUSIONS

The proposed work had the goal of develop and validate a new Python code using finite difference method. This was achieved comparing the results obtained thought Python simulation with Yau *et al*. (2012), using Matlab simulation and the commercial software Abacus 6.3. Using constants thermodynamic proprieties new cases were proposed with different mold material. This was made to investigate how the temperatures would be impacted by different proprieties. Concluding that the commercial materials are not adequate to be used in the cure rubber. Since their temperature profile, do not exhibit the same trend as the material used in the base cases.

Suggestions for feature works as follows:

- Explicit finite difference method was used, since it requires more computation processing and steps, it is suggested that an implicit former of the method used, generating fasters results.
- The thermodynamic proprieties used were consider as a constant, it is suggested that the code would account for their variation whit temperature.
- Future work should include shrinkage model and solve the more complicated equations about heat and mass transfer considering the water concentration variation to improve the formulated model. The inclusion of the vapor phase in the drying air would also help improve the physical model.

5. REFERENCES

Ajania C.; Curcioc S.; Dejchanchaiwonga R.; Tekasakul P.; 2019. "Influence of shrinkage during natural rubber sheet drying: Numerical modeling of heat and mass transfer", Applied Thermal Engineering, Vol 149, pp 798-806.

Dejchanchaiwong R.; Tirawanichakul Y.; Tirawanichakul S.; Kumar A.; Tekasakul P.; 2017. "Conjugate heat and mass transfer modeling of a new rubber smoking room and experimental validation", Applied Thermal Engineering, Vol 112, pp 761-770.

Dolkun D.; Zhu W.; Xu Q.; Ke Y., 2018. "Optimization of cure profile for thick composite parts based on finite element analysis and genetic algorithm". Journal of Composite Materials, Vol 52, pp 3885-3894.

Erfanian M.; Anbarsooz M.; Moghiman M., 2016. "A three dimensional simulation of a rubber curing process considering variable order of reaction". Applied Mathematical Modelling, Vol 40, pp 8592-8604.

Gregory, I.H., Alan, A.H., Iizan, A.B., 1999. "Prediction of state of cure throughout rubber components". Journal of Rubber Research, 2 (1).

Ghoreishy M.; 2016. "A state-of-the-art review on the mathematical modeling and computer simulation of rubber vulcanization process|". Iranian Polymer Journal, Vol 25, pp 89-109.

Incropera F.P.; Dewitt D.P.; Bergman T.; Lavine A.S.; 2007. Fundamentos da transferência de Calor e Massa. Jonh Wiley & Sons, New Jersey, 6th edition.

Julia, G.; 2007. " Cure optimisation using finite element analysis". Jornal of Rubber Research, 7 (1).

Kiusalaas, J. 2013. " Numerical Methods in Engineering with Python 3". Cambridge University Press, New York, 3nd edition

Lia F.; Liub F.; Liua J.; Gaoa Y.; Lub Y.; Chena J.; Yangb H.; Zhang L.; 2018. "Thermo-mechanical coupling analysis of transient temperature and rolling resistance for solid rubber tire: Numerical simulation and experimental verification", Composites Science and Technology, Vol 167, pp 404-410.

Limrungruengrat S.; Chaikittiratana A.; Pornpeerakeat S.; Chantrasmi T.; 2018. "Finite element analysis for evaluation of cure level in a large rubber part". Materials today: Proceedings, Vol 5, pp 9336-9343.

Luoa W.; Yina B.; Hua X.; Zhoua Z.; Denga Y.; Songa K.; 2018. "Modeling of the heat build-up of carbon black filled rubber", Polymer Testing, Vol 69, pp 116-124.

Rafei, M., Ghoreishy, H. R., Naderi, G., 2009. "Development of an advanced computer simulation technique for the modeling of rubber curing process". Computational Materials Science, Vol 47 (2), pp 539-547.

White, J.L., 2005. "Rheological Behavior and Processing of Unvulcanized Rubber". Science and Technology of Rubber, 3nd edition, pp 237-319

Yau Y.H.; Wong H.F.; Ahmad N.; 2012. "Numerical heat transfer study for a large rubber product". International Journal of Heat and Mass Transfer, Vol 55, pp 2879-2888.

6. ACKNOWLEDGMENTS

The last author would like to thank National Council of Scientific and Technologic Development of Brazil - CNPq (Grants number: 303906/2015-4-PQ, 405101/2016-3-Univ) and *Fundação Araucária* PRONEX Grant 042/2018 for its financial support of this work.

7. RESPONSIBILITY NOTICE

The authors are the only responsible for the printed material included in this paper.